

Electron-hydrogen scattering in Faddeev-Merkuriev integral equation approach

Z. Papp¹ and C.-Y. Hu²

¹ *Institute of Nuclear Research of the Hungarian Academy of Sciences, Debrecen, Hungary*

² *Department of Physics and Astronomy, California State University, Long Beach, 90840, California*

(Dated: October 24, 2018)

Electron-hydrogen scattering is studied in the Faddeev-Merkuriev integral equation approach. The equations are solved by using the Coulomb-Sturmian separable expansion technique. We present S - and P -wave scattering and reactions cross sections up to the $H(n = 4)$ threshold.

PACS numbers: 31.15.-p, 34.10.+x, 34.85.+x, 21.45.+v, 03.65.Nk, 02.30.Rz, 02.60.Nm

Introduction

The scattering of electrons on hydrogen atom is a fundamental three-body problem in atomic physics. The long-range Coulomb interaction presents the major difficulty. On the other hand, it is a special kind of Coulomb three-body problem as it contains two identical particles. While many studies have been carried out aiming at solving the Schrödinger equation using perturbative, close-coupling, variational or direct numerical methods approaches along to the Faddeev equations are relatively scarce. Here, by solving Faddeev-type integral equations, we present a general numerical method suitable for the treatment of elastic and inelastic processes in three-body Coulombic systems with two identical particles and apply the formalism for the electron-hydrogen system.

For quantum mechanical three-body systems the Faddeev integral equations are the fundamental equations. They possess connected kernels and therefore they are Fredholm-type integral equations of second kind. The Faddeev equations were derived for short range interactions and if we simply plug-in a Coulomb-like potential they become singular. The necessary modification were proposed by Merkuriev [1]. In Merkuriev's approach the Coulomb interactions were split into short-range and long-range parts. The long-range parts were included into the „free” Green's operators and the Faddeev procedure were performed only with the short-range potentials. The corresponding modified Faddeev, or Faddeev-Merkuriev equations are mathematically well-behaved. They possess compact kernels even in the case of attractive Coulombic interactions. This means that the Faddeev-Merkuriev equations possess all the nice properties of the original Faddeev equations.

However, the associated three-body Coulomb Green's operator is not known explicitly. To circumvent the problem the integral equations were cast into differential form and the appropriate boundary conditions were derived from the asymptotic analysis of the three-body Coulomb Green's operator. These modified Faddeev differential equations were successfully solved for various atomic three-body problems, including electron-hydrogen scattering up to the $H(n = 3)$ threshold [2].

A characteristic property of the atomic three body systems is that, due to attractive Coulomb interactions,

they have infinitely many two-body channels. If the total energy of the system increases more and more channels open up. The differential equation approach needs boundary conditions for each channels, and becomes intractable if the energy increases beyond a limit. Integral equations do not need boundary conditions, this information is incorporated in the Green's operators. They need initial conditions, which are much simpler. Therefore an integral equation approach to the three-body Coulomb problem would be very useful, it could provide an unified description of the scattering and reactions processes for all energies.

In the past few years we have developed a new approach to the three-body Coulomb problem. Faddeev-type integral equations were solved by using the Coulomb-Sturmian separable expansion method. The approach was developed first for solving the nuclear three-body scattering problem with repulsive Coulomb interactions [3], which has been adapted recently for atomic systems with attractive Coulomb interactions [4]. The basic concept in this method is a „three-potential” picture, where the S matrix is given in three terms. In this approach we solve the Faddeev-Merkuriev integral equations such that the associated three-body Coulomb Green's operator is calculated by an independent Lippmann-Schwinger-type integral equation. This Lippmann-Schwinger integral equation contains the channel-distorted Coulomb Green's operator, which can be calculated as a contour integral of two-body Coulomb Green's operators. The method were tested in positron-hydrogen scattering for energies up to the $H(n = 2) - Ps(n = 2)$ gap [4], and good agreements with the configuration-space solution of the Faddeev-Merkuriev equations were found.

In this paper we apply this formalism for the electron-hydrogen scattering problem. In Sec. I we briefly describe the Faddeev-Merkuriev integral equations, the details are given in Ref. [4]. However, the fact that in the electron-hydrogen system we have to deal with identical particles requires some additional considerations: the symmetry simplifies the numerical procedure. In Sec. II the integral equations are solved by the Coulomb-Sturmian separable expansion method. In Sec. III we show some test calculations up to the $H(n = 4)$ threshold with total angular momenta $L = 0$ and $L = 1$. Finally, we draw some conclusions.

I. FADDEEV-MERKURIEV INTEGRAL EQUATIONS FOR THE $e^- + H$ SYSTEM

In the $e^- + H$ system the two electrons are identical. Let us denote them by 1 and 2, and the non-identical proton by 3. The Hamiltonian is given by

$$H = H^0 + v_1^C + v_2^C + v_3^C, \quad (1)$$

where H^0 is the three-body kinetic energy operator and v_α^C denotes the Coulomb interaction in the subsystem α . We use the usual configuration-space Jacobi coordinates x_α and y_α , where x_α is the coordinate between the pair (β, γ) and y_α is the coordinate between the particle α and the center of mass of the pair (β, γ) . Thus the potential v_α^C , the interaction of the pair (β, γ) , appears as $v_\alpha^C(x_\alpha)$. The Hamiltonian (1) is defined in the three-body Hilbert space. So, the two-body potential operators are formally embedded in the three-body Hilbert space,

$$v^C = v^C(x)\mathbf{1}_y, \quad (2)$$

where $\mathbf{1}_y$ is a unit operator in the two-body Hilbert space associated with the y coordinate.

The role of a Coulomb potential in a three-body system is twofold. In one hand, it acts like a long-range potential since it modifies the asymptotic motion. On the other hand, however, it acts like a short-range potential, since it correlates strongly the particles and may support bound states. Merkuriev introduced a separation of the three-body configuration space into different asymptotic regions [1]. The two-body asymptotic region Ω is defined as a part of the three-body configuration space where the conditions

$$|x| < x_0(1 + |y|/y_0)^{1/\nu}, \quad (3)$$

with $x_0, y_0 > 0$ and $\nu > 2$, are satisfied. Merkuriev proposed to split the Coulomb interaction in the three-body configuration space into short-range and long-range terms

$$v^C = v^{(s)} + v^{(l)}, \quad (4)$$

where the superscripts s and l indicate the short- and long-range attributes, respectively. The splitting is carried out with the help of a splitting function ζ ,

$$v^{(s)}(x, y) = v^C(x)\zeta(x, y), \quad (5a)$$

$$v^{(l)}(x, y) = v^C(x)[1 - \zeta(x, y)]. \quad (5b)$$

The function ζ vanishes asymptotically within the three-body sector, where $x \sim y \rightarrow \infty$, and approaches one in the two-body asymptotic region Ω , where $x \ll y \rightarrow \infty$. Consequently in the three-body sector $v^{(s)}$ vanishes and $v^{(l)}$ approaches v^C . In practice usually the functional form

$$\zeta(x, y) = 2 / \{1 + \exp[(x/x_0)^\nu / (1 + y/y_0)]\}, \quad (6)$$

is used.

In the Hamiltonian (1) the Coulomb potential v_3^C , the interaction between the two electrons, is repulsive, and does not support bound states. Consequently, there are no two-body channels associated with this fragmentation. Therefore the entire v_3^C can be considered as long-range potential. Then, the long-range Hamiltonian is defined as

$$H^{(l)} = H^0 + v_1^{(l)} + v_2^{(l)} + v_3^C, \quad (7)$$

and the three-body Hamiltonian takes the form

$$H = H^{(l)} + v_1^{(s)} + v_2^{(s)}. \quad (8)$$

So, the Hamiltonian (8) appears formally as a three-body Hamiltonian with two short-range potentials. The bound-state wave function $|\Psi\rangle$ satisfies the homogeneous Lippmann-Schwinger integral equation

$$|\Psi\rangle = G^{(l)} [v_1^{(s)} + v_2^{(s)}] |\Psi\rangle = G^{(l)} v_1^{(s)} |\Psi\rangle + G^{(l)} v_2^{(s)} |\Psi\rangle, \quad (9)$$

where $G^{(l)}(z) = (z - H^{(l)})^{-1}$ is the resolvent operator of $H^{(l)}$. This induce, in the spirit of the Faddeev procedure, the splitting of the wave function $|\Psi\rangle$ into two components

$$|\Psi\rangle = |\psi_1\rangle + |\psi_2\rangle, \quad (10)$$

where the components are defined by

$$|\psi_\alpha\rangle = G^{(l)} v_\alpha^{(s)} |\Psi\rangle, \quad (11)$$

with $\alpha = 1, 2$. The components satisfy the set of two-component Faddeev-Merkuriev integral equations

$$|\psi_1\rangle = |\Phi_1^{(l)}\rangle + G_1^{(l)} v_1^{(s)} |\psi_2\rangle \quad (12a)$$

$$|\psi_2\rangle = G_2^{(l)} v_2^{(s)} |\psi_1\rangle, \quad (12b)$$

where $G_\alpha^{(l)}$ is the resolvent operator of the channel Coulomb Hamiltonian

$$H_\alpha^{(l)} = H^{(l)} + v_\alpha^{(s)} \quad (13)$$

and the inhomogeneous term $|\Phi_1^{(l)}\rangle$ is an eigenstate of $H_1^{(l)}$.

Before going further let us examine the spectral properties of the Hamiltonian

$$H_1^{(l)} = H^{(l)} + v_1^{(s)} = H^0 + v_1^C + v_2^{(l)} + v_3^C. \quad (14)$$

It obviously supports infinitely many two-body channels associated with the bound states of the attractive Coulomb potential v_1^C . The potential v_3^C is repulsive and does not have bound states. The three-body potential $v_2^{(l)}$ is attractive and constructed such that $v_2^{(l)}(x_2, y_2) \rightarrow 0$ if $y_2 \rightarrow \infty$. Therefore, there are no two-body channels associated with fragmentations 2 and 3,

the Hamiltonian $H_1^{(l)}$ has only 1-type two-body asymptotic channels. Consequently, the corresponding $G_1^{(l)}$ Green's operator, acting on the $v_1^{(s)}|\psi_2\rangle$ term in (12a), will generate only 1-type two-body asymptotic channels in $|\psi_1\rangle$. Similar analysis is valid also for $|\psi_2\rangle$. Thus, the Faddeev-Merkuriev procedure results in the separation of the three-body wave function into components such a way that each component has only one type of two-body asymptotic channels. This is the main advantage of the Faddeev equations and, as this analysis shows, this property remains true also for attractive Coulomb potentials if the Merkuriev splitting is adopted.

In the e^-e^-p system the particles 1 and 2, the two electrons, are identical and indistinguishable. Therefore, the Faddeev components $|\psi_1\rangle$ and $|\psi_2\rangle$, in their own natural Jacobi coordinates, should have the same functional forms

$$\langle x_1 y_1 | \psi_1 \rangle = \langle x_2 y_2 | \psi_2 \rangle = \langle xy | \psi \rangle. \quad (15)$$

On the other hand, by interchanging the two electrons we have

$$\mathcal{P}|\psi_1\rangle = p|\psi_2\rangle, \quad (16)$$

where the operator \mathcal{P} describes the exchange of particles 1 and 2, and $p = \pm 1$ is the eigenvalue of \mathcal{P} . Building this information into the formalism results the integral equation

$$|\psi\rangle = |\Phi_1^{(l)}\rangle + G_1^{(l)} v_1^{(s)} p \mathcal{P} |\psi\rangle, \quad (17)$$

which is alone sufficient to determine $|\psi\rangle$. We notice that so far no approximation has been made, and although this Faddeev-Merkuriev integral equation has only one component, yet it gives a full account on the asymptotic and symmetry properties of the system.

II. COULOMB-STURMIAN SEPARABLE EXPANSION APPROACH

We solve this integral equation by applying the Coulomb-Sturmian separable expansion approach. This approach has been established in a series of papers for two- [5] and three-body [3, 4, 6] problems with Coulomb-like potentials. The Coulomb-Sturmian (CS) functions are defined by

$$\langle r | nl \rangle = \left[\frac{n!}{(n+2l+1)!} \right]^{1/2} (2br)^{l+1} \exp(-br) L_n^{2l+1}(2br), \quad (18)$$

with n and l being the radial and orbital angular momentum quantum numbers, respectively, and b is the size parameter of the basis. The CS functions $\{|nl\rangle\}$ form a biorthonormal discrete basis in the radial two-body Hilbert space; the biorthogonal partner defined by $\langle r | nl \rangle = \langle r | nl \rangle / r$.

Since the three-body Hilbert space is a direct product of two-body Hilbert spaces an appropriate basis is the bipolar basis, which can be defined as the angular momentum coupled direct product of the two-body bases,

$$|n\nu l \lambda\rangle_\alpha = |nl\rangle_\alpha \otimes |\nu\lambda\rangle_\alpha, \quad (n, \nu = 0, 1, 2, \dots), \quad (19)$$

where $|nl\rangle_\alpha$ and $|\nu\lambda\rangle_\alpha$ are associated with the coordinates x_α and y_α , respectively. With this basis the completeness relation takes the form (with angular momentum summation implicitly included)

$$\mathbf{1} = \lim_{N \rightarrow \infty} \sum_{n, \nu=0}^N |\widetilde{n\nu l \lambda}\rangle_\alpha \langle n\nu l \lambda| = \lim_{N \rightarrow \infty} \mathbf{1}_\alpha^N, \quad (20)$$

where $\langle xy | \widetilde{n\nu l \lambda} \rangle = \langle xy | n\nu l \lambda \rangle / (xy)$.

We make the following approximation on the integral equation (17)

$$|\psi\rangle = |\Phi_1^{(l)}\rangle + G_1^{(l)} \mathbf{1}_1^N v_1^{(s)} p \mathcal{P} \mathbf{1}_1^N |\psi\rangle, \quad (21)$$

i.e. the operator $v_1^{(s)} p \mathcal{P}$ is approximated in the three-body Hilbert space by a separable form, viz.

$$\begin{aligned} v_1^{(s)} p \mathcal{P} &= \lim_{N \rightarrow \infty} \mathbf{1}_1^N v_1^{(s)} p \mathcal{P} \mathbf{1}_1^N \\ &\approx \mathbf{1}_1^N v_1^{(s)} p \mathcal{P} \mathbf{1}_1^N \\ &\approx \sum_{n, \nu, n', \nu'=0}^N |\widetilde{n\nu l \lambda}\rangle_1 \underline{v}_1^{(s)} \langle n' \nu' l' \lambda' |, \end{aligned} \quad (22)$$

where $\underline{v}_1^{(s)} = \langle n\nu l \lambda | v_1^{(s)} p \mathcal{P} | n' \nu' l' \lambda' \rangle_1$. Utilizing the properties of the exchange operator \mathcal{P} these matrix elements can be written in the form $\underline{v}_1^{(s)} = p \times (-)^{l'} \langle n\nu l \lambda | v_1^{(s)} | n' \nu' l' \lambda' \rangle_2$, and can be evaluated numerically by using the transformation of the Jacobi coordinates [7]. The completeness of the CS basis guarantees the convergence of the method with increasing N and angular momentum channels.

Now, by applying the bra $\langle n'' \nu'' l'' \lambda'' |$ on Eq. (21) from left, the solution of the inhomogeneous Faddeev-Merkuriev equation turns into the solution of a matrix equation for the component vector $\underline{\psi} = \langle n\nu l \lambda | \psi \rangle$

$$\underline{\psi} = \underline{\Phi}_1^{(l)} + \underline{G}_1^{(l)} \underline{v}_1^{(s)} \underline{\psi}, \quad (23)$$

where

$$\underline{\Phi}_1^{(l)} = \langle n\nu l \lambda | \Phi_1^{(l)} \rangle \quad (24)$$

and

$$\underline{G}_1^{(l)} = \langle n\nu l \lambda | G_1^{(l)} | n' \nu' l' \lambda' \rangle_1. \quad (25)$$

The formal solution of Eq. (23) is given by

$$\underline{\psi} = [(\underline{G}_1^{(l)})^{-1} - \underline{v}_1^{(s)}]^{-1} (\underline{G}_1^{(l)})^{-1} \underline{\Phi}_1^{(l)}. \quad (26)$$

Unfortunately neither $\underline{G}_1^{(l)}$ nor $\underline{\Phi}_1^{(l)}$ are known. They are related to the Hamiltonian $H_1^{(l)}$, which is still a complicated three-body Coulomb Hamiltonian. The approximation scheme for $\underline{G}_1^{(l)}$ and $\underline{\Phi}_1^{(l)}$ is presented in Ref. [4]. Starting from the resolvent relation

$$G_1^{(l)} = \tilde{G}_1 + \tilde{G}_1 U_1 G_1^{(l)}, \quad (27)$$

where \tilde{G}_1 is the resolvent operator of the Hamiltonian

$$\tilde{H}_1 = H^0 + v_1^C \quad (28)$$

and the potential U_1 is defined by

$$U_1 = v_2^{(l)} + v_3^C, \quad (29)$$

for the CS matrix elements $(\underline{G}_1^{(l)})^{-1}$ we get

$$(\underline{G}_1^{(l)})^{-1} = (\tilde{\underline{G}}_1)^{-1} - \underline{U}_1, \quad (30)$$

where

$$\tilde{\underline{G}}_1 = {}_1\langle n\nu l\lambda | \tilde{G}_1 | n'\nu' l'\lambda' \rangle_1 \quad (31)$$

and

$$\underline{U}_1 = {}_1\langle n\nu l\lambda | U_1 | n'\nu' l'\lambda' \rangle_1. \quad (32)$$

These latter matrix elements can again be evaluated numerically.

Similarly, also the wave function $|\Phi_1^{(l)}\rangle$, a scattering eigenstate of $H_1^{(l)}$, satisfies the Lippmann-Schwinger equation

$$|\Phi_1^{(l)}\rangle = |\tilde{\Phi}_1\rangle + \tilde{G}_1 U_1 |\Phi_1^{(l)}\rangle, \quad (33)$$

where $|\tilde{\Phi}_1\rangle$ is an eigenstate of \tilde{H}_1 . The solution is given by

$$\underline{\Phi}_1^{(l)} = [(\tilde{\underline{G}}_1)^{-1} - \underline{U}_1]^{-1} (\tilde{\underline{G}}_1)^{-1} \tilde{\underline{\Phi}}_1, \quad (34)$$

where $\tilde{\underline{\Phi}}_1 = {}_1\langle n\nu l\lambda | \tilde{\Phi}_1 \rangle$.

The three-particle free Hamiltonian can be written as a sum of two-particle free Hamiltonians

$$H^0 = h_{x_1}^0 + h_{y_1}^0. \quad (35)$$

Consequently the Hamiltonian \tilde{H}_1 of Eq. (28) appears as a sum of two two-body Hamiltonians acting on different coordinates

$$\tilde{H}_1 = h_{x_1} + h_{y_1}, \quad (36)$$

with $h_{x_1} = h_{x_1}^0 + v_1^C(x_1)$ and $h_{y_1} = h_{y_1}^0$, which, of course, commute. Therefore the eigenstates of \tilde{H}_1 , in CS representation, are given by

$${}_1\langle n\nu l\lambda | \tilde{\Phi}_1 \rangle = {}_1\langle n l | \phi_1 \rangle \times {}_1\langle \nu \lambda | \chi_1 \rangle, \quad (37)$$

where $|\phi_1\rangle$ and $|\chi_1\rangle$ are bound and scattering eigenstates of h_{x_1} and h_{y_1} , respectively. The CS matrix elements of the two-body bound and scattering states $\langle n l | \phi \rangle$ and $\langle \nu \lambda | \chi \rangle$, respectively, are known analytically from the two-body case [5].

The most crucial point in this procedure is the calculation of the matrix elements $\tilde{\underline{G}}_1$. The Green's operator \tilde{G}_1 is a resolvent of the sum of two commuting Hamiltonians. Thus, according to the convolution theorem, the three-body Green's operator \tilde{G}_1 equates to a convolution integral of two-body Green's operators, i.e.

$$\tilde{G}_1(z) = \frac{1}{2\pi i} \oint_C dz' g_{x_1}(z-z') g_{y_1}(z'), \quad (38)$$

where $g_{x_1}(z) = (z - h_{x_1})^{-1}$ and $g_{y_1}(z) = (z - h_{y_1})^{-1}$. The contour C should be taken counterclockwise around the singularities of g_{y_1} such a way that g_{x_1} is analytic on the domain encircled by C .

In the time-independent scattering theory the Green's operator has a branch-cut singularity at scattering energies. In our formalism $\tilde{G}_1(E)$ should be understood as $\tilde{G}_1(E) = \lim_{\varepsilon \rightarrow 0} \tilde{G}_1(E + i\varepsilon)$, with $\varepsilon > 0$, and $E < 0$, since in this work we are considering scattering below the three-body breakup threshold. To examine the analytic structure of the integrand in Eq. (38) let us take ε finite. By doing so, the singularities of g_{x_1} and g_{y_1} become well separated. In fact, g_{y_1} is a free Green's operator with branch-cut on the $[0, \infty)$ interval, while $g_{x_1}(E + i\varepsilon - z')$ is a Coulomb Green's operator, which, as function of z' , has a branch-cut on the $(-\infty, E + i\varepsilon]$ interval and infinitely many poles accumulated at $E + i\varepsilon$. Now, the branch cut of g_{y_1} can easily be encircled such that the singularities of g_{x_1} lie outside the encircled domain (Fig. 1). However, this would not be the case in the $\varepsilon \rightarrow 0$ limit. Therefore the contour C is deformed analytically such that the upper part descends into the unphysical Riemann sheet of g_{y_1} , while the lower part of C is detoured away from the cut (Fig. 2). The contour in Fig. 2 is achieved by deforming analytically the one in Fig. 1, but now, even in the $\varepsilon \rightarrow 0$ limit, the contour in Fig. 2 avoids the singularities of g_{x_1} . Thus, with the contour in Fig. 2 the mathematical conditions for the contour integral representation of \tilde{G}_1 in Eq. (38) is met also for scattering-state energies. The matrix elements $\tilde{\underline{G}}_1$ can be cast into the form

$$\tilde{\underline{G}}_1(E) = \frac{1}{2\pi i} \oint_C dz' \underline{g}_{x_1}(E - z') \underline{g}_{y_1}(z'), \quad (39)$$

where the corresponding CS matrix elements of the two-body Green's operators in the integrand are known analytically for all complex energies [4, 5].

In the three-potential formalism [3, 4] the S matrix can be decomposed into three terms. The first one describes a single channel Coulomb scattering, the second one is a multichannel two-body-type scattering due to the potential U , and the third one is a genuine three-body scattering. In our $e^- + H$ case the target is neutral

and the first term is absent. For the on-shell T matrix we have

$$T_{fi} = \sqrt{\frac{\mu_f \mu_i}{k_f k_i}} \left(\langle \tilde{\Phi}_{1f}^{(-)} | U_1 | \Phi_{1i}^{(l)(+)} \rangle + \langle \Phi_{1f}^{(l)(-)} | v_1^{(s)} | \psi_{2i}^{(+)} \rangle \right), \quad (40)$$

where i and f refer to the initial and the final states, respectively, μ is the channel reduced mass and k is the channel wave number. Having the solutions $\underline{\psi}$ and $\underline{\Phi}^{(l)}$ and the matrix elements \underline{U}_1 and $\underline{v}_1^{(s)}$, the T matrix elements can easily be evaluated. The spin-weighted cross section of the transition $i \rightarrow f$ is given by

$$\sigma_{fi} = \frac{\pi a_0^2}{k_i^2} \frac{(2S_{12} + 1)(2L + 1)}{(2l_i + 1)} |T_{fi}|^2, \quad (41)$$

where a_0 is the Bohr radius, L is the total angular momentum, S_{12} is the total spin of the two electrons and l_i is the angular momentum of the target hydrogen atom.

III. RESULTS

In the numerical calculations we use atomic units (the mass of the electrons $m_1 = m_2 = 1$ and the mass of the proton $m_3 = 1836.151527$). In this paper we are concerned with total angular momenta $L = 0$ and $L = 1$. The formula (40) gives some hint for the choice of the parameters in the splitting function ζ . We can expect good convergence if the "size" of $v_1^{(s)}$ corresponds to the "size" of $\Phi_{1f}^{(l)(-)}$. Therefore we may need to adjust the parameters of the splitting function if we consider more and more open channels. Consequently, we also need to adjust the b parameter of the CS basis. We found that the final results and the rate of the convergence does not depend on the choice of b , within a rather broad interval around the optimal value.

Having the T matrix we can also calculate the K matrix, whose symmetry, which is equivalent to the unitarity of the S matrix, provides a delicate and independent test of the method. We observed that if either the parameters of the splitting function are too far from the optimum or the convergence with the basis is not achieved the K matrix fails to be symmetric. In the separable expansion we take up to 9 bipolar angular momentum channels with CS functions up to $N = 36$. This requires solution of complex general matrix equations with maximal size of 12321×12321 , a problem which can even be handled on a workstation. We need relatively small basis because in this approach we approximate only short-range type potentials and the correct asymptotic is guaranteed by the Green's operators.

We present first our S -wave results for energies below the $H(n = 2)$ threshold. In this energy region we use parameters $\nu = 2.1$, $x_0 = 3$, $y_0 = 20$ and $b = 0.6$. Table I shows elastic phase shifts at several values of electron

momenta k_1 . Our results, which was achieved by using finite proton mass, agree very well with variational calculations of Ref. [8], R -matrix calculations of Ref. [9], finite-element method of Ref. [10], as well as with the results of direct numerical solution of the Schrödinger equation of Ref. [11], where infinite mass for proton were adopted. We also compare our calculation with the differential equation solution of the modified Faddeev equations [2]. We can observe perfect agreements with all the previous calculations.

In Table II we present S -wave partial cross sections and K matrices between the $H(n = 2) - H(n = 3)$ thresholds at channel energy $E_1 = 0.81\text{Ry}$ and for $L = 0$, where we have 3 open channels. We used parameters $\nu = 2.1$, $x_0 = 3.5$, $y_0 = 20$ and $b = 0.3$. For comparison we also show the results of a configuration-space Faddeev calculation [12]. We can report perfect agreements not only for the cross sections but also for the K matrix (except for an unphysical phase factor). Our cross sections are also in a good agreements with the results of Ref. [11].

In Tables III we show the S -wave K matrix between the $H(n = 3) - H(n = 4)$ thresholds at channel energy $E_1 = 0.93\text{Ry}$, where we have 6 open channels. We used parameters $\nu = 2.1$, $x_0 = 4$, $y_0 = 20$ and $b = 0.2$. We can see that the K matrix is nearly perfectly symmetric. In Tables IV we present S -wave partial cross sections between the $H(n = 3) - H(n = 4)$ thresholds at channel energies $E_1 = 0.93\text{Ry}$, $E_1 = 0.91\text{Ry}$ and $E_1 = 0.89\text{Ry}$, respectively. In Tables V-VIII we present the corresponding P -wave K matrices and cross sections.

IV. SUMMARY

In this work we have studied electron-hydrogen scattering problem by solving the Faddeev-Merkuriev integral equations. In this particular case, where two particles are identical, the Faddeev scheme results in an one-component equation, which, however, gives full account on the asymptotic and symmetry properties of the system. We solved the integral equations by applying the Coulomb-Sturmian separable expansion method.

We calculated S - and P -wave scattering and reaction cross sections for energies up to the $H(n = 4)$ threshold. Our nearly perfectly symmetric K matrices indicate that in our approach all the fine details of the scattering processes are properly taken into account.

Acknowledgments

This work has been supported by the NSF Grant No. Phy-0088936 and by the OTKA Grants No. T026233 and No. T029003. We are thankful to the Aerospace Engineering Department of CSULB for the generous allocation of computer resources.

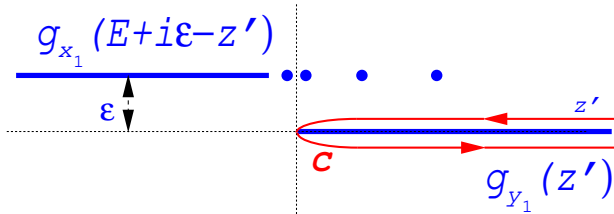


FIG. 1: Analytic structure of $g_{x_1}(E+i\epsilon-z')$ $g_{y_1}(z')$ as a function of z' , $\epsilon > 0$. The Green's operator $g_{y_1}(z')$ has a branch-cut on the $[0, \infty)$ interval, while $g_{x_1}(E+i\epsilon-z')$ has a branch-cut on the $(-\infty, E+i\epsilon]$ interval and infinitely many poles accumulated at $E+i\epsilon$ (denoted by dots). The contour C encircles the branch-cut of g_{y_1} . In the $\epsilon \rightarrow 0$ limit the singularities of $g_{x_1}(E+i\epsilon-z')$ would penetrate into the area covered by C .

- [1] S. P. Merkuriev, Ann. Phys. NY, **130**, 395, (1980); L. D. Faddeev and S. P. Merkuriev, *Quantum Scattering Theory for Several Particle Systems*, (Kluwer, Dordrecht,1993).
 [2] A. A. Kvitsinsky, A. Wu, and C.-Y. Hu, J. Phys. B: At.

- Mol. Opt. Phys. **28** 275 (1995).
 [3] Z. Papp, Phys. Rev. C **55**, 1080 (1997).
 [4] Z. Papp, C.-Y. Hu, Z. T. Hlousek, B. Kónya and S. L. Yakovlev, Phys. Rev. A, (2001).
 [5] Z. Papp, J. Phys. A **20**, 153 (1987); Z. Papp, Phys. Rev. C **38**, 2457 (1988); Z. Papp, Phys. Rev. A **46**, 4437 (1992); Z. Papp, Comput. Phys. Commun. **70**, 426 (1992); Z. Papp, Comput. Phys. Commun. **70**, 435 (1992); B. Kónya, G. Lévai, and Z. Papp, Phys. Rev. C **61**, 034302 (2000).
 [6] Z. Papp and W. Plessas, Phys. Rev. C **54**, 50 (1996); Z. Papp, Few-Body Systems, **24** 263 (1998).
 [7] R. Balian and E. Brézin, Nuovo Cim. B **2**, 403 (1969).
 [8] C. Schwartz, Phys. Rev. **124**, 553 (1961).
 [9] T. Scholz, P. Scott and P. G. Burke, J. Phys. B: At. Mol. Opt. Phys. **21**, L139 (1988).
 [10] J. Botero and J. Shertzer, Phys. Rev. A **46**, R1155 (1992).
 [11] Y. D. Wang and J. Callaway, Phys. Rev. A **48**, 2058 (1993); Phys. Rev. A **50**, 2327 (1994).
 [12] C.-Y. Hu, J. Phys. B: At. Mol. Opt. Phys. **32**, 3077 (1999); Phys. Rev. A **59**, 4813 (1999).

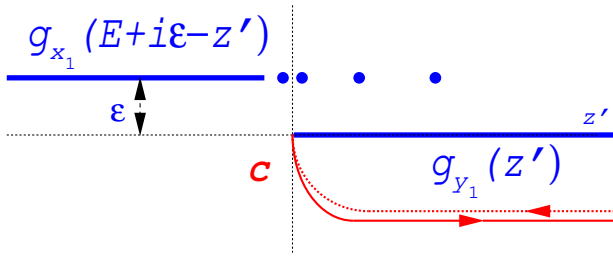


FIG. 2: The contour of Fig. 1 is deformed analytically such that a part of it goes on the unphysical Riemann-sheet of g_{y_1} (drawn by broken line) and the other part detoured away from the cut. Now, the contour avoids the singularities of $g_{x_1}(E+i\epsilon-z')$ even in the $\epsilon \rightarrow 0$ limit.

TABLE I: Singlet ($^1S^e, p = +1$) and triplet ($^3S^e, p = -1$) phase shifts of elastic S -wave $e^- + H$ scattering .

k	Ref. [8]	Ref. [9]	Ref. [10]	Ref. [11]	Ref. [2]	This work
$^1S^e, p = +1$						
0.1	2.553	2.550	2.553	2.555	2.553	2.552
0.2	2.0673	2.062	2.066	2.066	2.065	2.064
0.3	1.6964	1.691	1.695	1.695	1.694	1.693
0.4	1.4146	1.410	1.414	1.415	1.415	1.412
0.5	1.202	1.196	1.202	1.200	1.200	1.197
0.6	1.041	1.035	1.040	1.041	1.040	1.037
0.7	0.930	0.925	0.930	0.930	0.930	0.927
0.8	0.886		0.887	0.887	0.885	0.884
$^3S^e, p = -1$						
0.1	2.9388	2.939	2.938	2.939	2.939	2.938
0.2	2.7171	2.717	2.717	2.717	2.717	2.717
0.3	2.4996	2.500	2.500	2.500	2.499	2.499
0.4	2.2938	2.294	2.294	2.294	2.294	2.294
0.5	2.1046	2.105	2.104	2.104	2.105	2.104
0.6	1.9329	1.933	1.933	1.933	1.933	1.932
0.7	1.7797	1.780	1.780	1.780	1.779	1.779
0.8	1.643		1.645	1.644	1.641	1.643

TABLE II: $L = 0$ partial cross sections (in πa_0^2) in the $H(n = 2) - H(n = 3)$ gap at channel energy $E_1 = 0.81\text{Ry}$. Channel numbers 1, 2 and 3 refer to the channels $e^- + H(1s)$, $e^- + H(2s)$ and $e^- + H(2p)$, respectively. For comparison the result of a configuration-space Faddeev calculation is presented.

Ch.#	1	2	3	
$^1S^e, p = +1$				
This work				
σ_{ij}	1	0.564	0.061	0.024
	2	0.817	8.373	2.588
	3	0.107	0.863	1.722
K_{ij}	1	1.895	-2.036	1.792
	2	-2.043	5.230	-4.114
	3	1.798	-4.114	2.366
Method of Ref. [12]				
σ_{ij}	1	0.568	0.061	0.024
	2	0.814	8.720	2.471
	3	0.105	0.824	1.697
K_{ij}	1	1.864	1.971	-1.671
	2	1.980	5.131	-3.843
	3	-1.679	-3.843	2.028
$^3S^e, p = -1$				
This work				
σ_{ij}	1	3.694	0.001	0.0006
	2	0.016	10.04	1.641
	3	0.003	0.547	11.85
K_{ij}	1	21.34	0.3255	0.6386
	2	0.3268	-0.4404	-0.4161
	3	0.6409	-0.4161	1.755
Method of Ref. [12]				
σ_{ij}	1	3.696	0.001	0.0006
	2	0.016	10.20	1.678
	3	0.003	0.560	11.77
K_{ij}	1	24.76	-0.3823	-0.7510
	2	-0.3803	-0.4441	-0.4167
	3	-0.7453	-0.4165	1.737

TABLE III: S -wave K matrices in the $H(n=3) - H(n=4)$ gap at channel energy $E_1 = 0.93\text{Ry}$. The channel numbers 1, 2, 3, 4, 5 and 6 refer to the channels $e^-(\lambda=0) + H(1s)$, $e^-(\lambda=0) + H(2s)$, $e^-(\lambda=0) + H(3s)$, $e^-(\lambda=1) + H(1p)$, $e^-(\lambda=1) + H(2p)$ and $e^-(\lambda=2) + H(1d)$, respectively.

Ch.#	1	2	3	4	5	6
$E_1 = 0.93\text{Ry}, {}^1S^e, p = +1$						
1	1.076	-0.647	-0.160	0.229	0.180	0.074
2	-0.652	1.541	-0.028	0.129	0.531	0.265
3	-0.160	-0.029	0.766	0.314	-0.757	-0.385
4	0.230	0.130	0.314	-0.566	-0.525	-0.284
5	0.180	0.534	-0.757	-0.526	0.237	0.760
6	0.074	0.266	-0.385	-0.285	0.760	1.342
$E_1 = 0.93\text{Ry}, {}^3S^e, p = -1$						
1	9.054	0.507	0.019	0.666	0.099	0.028
2	0.543	-1.700	-0.111	-1.530	-0.113	-0.120
3	0.025	-0.112	0.155	-0.050	-0.926	-0.070
4	0.702	-1.532	-0.050	-0.851	-0.253	-0.048
5	0.104	-0.114	-0.926	-0.253	0.927	0.449
6	0.030	-0.120	-0.070	-0.049	0.449	-0.111

TABLE IV: $L = 0$ partial cross sections (in πa_0^2) in the $H(n = 3) - H(n = 4)$ gap at channel energies $E_1 = 0.93\text{Ry}$, $E_1 = 0.91\text{Ry}$ and $E_1 = 0.89\text{Ry}$, respectively. The channel numbers 1, 2, 3, 4, 5 and 6 refer to the channels $e^-(\lambda = 0) + H(1s)$, $e^-(\lambda = 0) + H(2s)$, $e^-(\lambda = 0) + H(3s)$, $e^-(\lambda = 1) + H(1p)$, $e^-(\lambda = 1) + H(2p)$ and $e^-(\lambda = 2) + H(1d)$, respectively.

Ch.#	1	2	3	4	5	6
$E_1 = 0.93\text{Ry}, {}^1S^e, p = +1$						
1	0.44	0.48(-1)	0.67(-2)	0.28(-1)	0.86(-2)	0.20(-2)
2	0.25	3.02	0.19(-1)	0.10	0.12	0.40(-1)
3	0.15	0.83(-1)	4.68	0.71	2.41	0.86
4	0.49(-1)	0.34(-1)	0.55(-1)	0.49	0.59(-1)	0.24(-1)
5	0.65(-1)	0.18	0.80	0.26	1.48	0.44
6	0.89(-2)	0.35(-1)	0.17	0.61(-1)	0.27	2.0
$E_1 = 0.93\text{Ry}, {}^3S^e, p = -1$						
1	3.18	0.22(-2)	0.43(-4)	0.21(-2)	0.26(-4)	0.14(-5)
2	0.12(-1)	5.92	0.93(-2)	3.77	0.44(-1)	0.61(-1)
3	0.97(-3)	0.40(-1)	7.56	0.35	11.6	3.34
4	0.39(-2)	1.26	0.26(-1)	0.87	0.11(-1)	0.19(-2)
5	0.23(-3)	0.63(-1)	3.87	0.48(-1)	9.14	1.07
6	0.79(-5)	0.53(-1)	0.67	0.49(-2)	0.64	0.34
$E_1 = 0.91\text{Ry}, {}^1S^e, p = +1$						
1	0.46	0.45(-1)	0.90(-2)	0.24(-1)	0.89(-2)	0.18(-2)
2	0.26	3.74	0.24	0.77(-1)	0.74(-1)	0.15(-1)
3	0.38	1.77	5.46	1.11	0.90	1.14
4	0.46(-1)	0.26(-1)	0.50(-1)	0.49	0.86(-1)	0.30(-1)
5	0.13	0.18	0.30	0.64	11.5	0.37
6	0.16(-1)	0.23(-1)	0.23	0.13	0.22	1.15
$E_1 = 0.91\text{Ry}, {}^3S^e, p = -1$						
1	3.26	0.22(-2)	0.23(-4)	0.20(-2)	0.20(-4)	0.17(-5)
2	0.13(-1)	7.22	0.24(-1)	4.07	0.28(-1)	0.25(-1)
3	0.96(-3)	0.18	9.11	0.33	0.27	12.25
4	0.37(-2)	1.36	0.15(-1)	0.98	0.10(-1)	0.31(-2)
5	0.26(-3)	0.69(-1)	0.89(-1)	0.74(-1)	44.97	0.44
6	0.14(-4)	0.38(-1)	2.45	0.14(-1)	0.27	2.81
$E_1 = 0.89\text{Ry}, {}^1S^e, p = +1$						
1	0.48	0.47(-1)	0.53(-2)	0.21(-1)	0.79(-2)	0.26(-2)
2	0.30	4.67	0.32(-1)	0.61(-1)	0.14	0.12
3	2.98	2.80	259.8	19.02	1.58	7.12
4	0.45(-1)	0.20(-1)	0.72(-1)	0.51	0.77(-1)	0.13(-1)
5	1.48	3.40	0.53	6.78	119.8	2.67
6	0.29	2.04	1.42	0.70	1.60	38.90
$E_1 = 0.91\text{Ry}, {}^3S^e, p = -1$						
1	3.34	0.22(-2)	0.67(-5)	0.17(-2)	0.90(-5)	0.25(-5)
2	0.13(-1)	8.68	0.94(-2)	4.33	0.17(-1)	0.87(-1)
3	0.37(-3)	0.83	1321.0	1.75	152.8	58.26
4	0.33(-2)	1.44	0.66(-2)	1.25	0.67(-2)	0.12(-2)
5	0.16(-2)	0.49	50.93	0.59	124.6	56.47
6	0.25(-3)	0.15	11.65	0.63(-1)	33.88	218.4

TABLE V: P -wave K matrices in the $H(n=3) - H(n=4)$ gap at channel energy $E_1 = 0.93\text{Ry}$. The channel numbers 1, 2, 3, 4, 5, 6, 7, 8 and 9 refer to the channels $e^-(\lambda=1) + H(1s)$, $e^-(\lambda=1) + H(2s)$, $e^-(\lambda=1) + H(3s)$, $e^-(\lambda=0) + H(2p)$, $e^-(\lambda=0) + H(3p)$, $e^-(\lambda=2) + H(2p)$, $e^-(\lambda=2) + H(3p)$, $e^-(\lambda=1) + H(3d)$ and $e^-(\lambda=3) + H(3d)$, respectively.

Ch.#	1	2	3	4	5	6	7	8	9
$E_1 = 0.93\text{Ry}, {}^1S^e, p = +1$									
1	-1.888	-7.518	13.24	9.699	8.320	7.148	1.992	4.684	30.96
2	-7.525	-29.70	51.80	38.14	32.73	28.88	7.839	18.28	121.5
3	13.30	51.99	-89.98	-67.93	-56.77	-50.01	-13.90	-29.57	-216.6
4	9.665	37.98	-67.40	-48.21	-42.35	-36.39	-9.947	-24.07	-156.7
5	8.346	32.81	-56.70	-42.64	-36.30	-31.16	-9.349	-19.40	-136.0
6	7.151	28.87	-49.82	-36.54	-31.08	-28.11	-7.718	-17.41	-117.3
7	2.006	7.885	-13.94	-10.05	-9.381	-7.765	-2.651	-4.874	-34.08
8	4.755	18.64	-29.92	-24.51	-19.64	-17.67	-4.915	-8.953	-73.21
9	31.01	121.6	-215.9	-157.5	-135.7	-117.3	-33.89	-72.15	-510.6
$E_1 = 0.93\text{Ry}, {}^3S^e, p = -1$									
1	0.454	-0.303	-0.051	-0.020	0.080	0.043	-0.017	0.149	0.128
2	-0.301	-2.453	-0.669	0.383	0.552	1.112	0.017	1.145	1.060
3	-0.051	-0.672	0.398	-0.465	1.140	-0.371	0.0001	0.578	0.486
4	-0.020	0.382	-0.464	0.354	-1.133	-0.236	0.883	-0.528	-0.110
5	0.079	0.553	1.137	-1.136	3.936	-0.699	-3.202	1.075	-0.989
6	0.041	1.113	-0.372	-0.236	-0.701	0.289	0.520	-0.769	-0.456
7	-0.016	0.018	0.002	0.884	-3.203	0.518	1.673	-1.484	-0.226
8	0.148	1.147	0.576	-0.530	1.075	-0.769	-1.483	-0.055	-0.278
9	0.127	1.062	0.486	-0.111	-0.988	-0.457	-0.226	-0.277	0.090

TABLE VI: $L = 1$ partial cross sections (in πa_0^2 unit) in the $H(n=3) - H(n=4)$ gap at channel energy $E_1 = 0.93\text{Ry}$. The channel numbers 1, 2, 3, 4, 5, 6, 7, 8 and 9 refer to the channels $e^-(\lambda=1) + H(1s)$, $e^-(\lambda=1) + H(2s)$, $e^-(\lambda=1) + H(3s)$, $e^-(\lambda=0) + H(2p)$, $e^-(\lambda=0) + H(3p)$, $e^-(\lambda=2) + H(2p)$, $e^-(\lambda=2) + H(3p)$, $e^-(\lambda=1) + H(3d)$ and $e^-(\lambda=3) + H(3d)$, respectively.

Ch.#	1	2	3	4	5	6	7	8	9
$E_1 = 0.93\text{Ry}, {}^1S^e, p = +1$									
1	0.380(-2)	0.104(-1)	0.138(-2)	0.394(-1)	0.677(-2)	0.125(-1)	0.543(-2)	0.664(-2)	0.180(-2)
2	0.530(-1)	0.208(1)	0.760(-2)	0.152(1)	0.139	0.135(1)	0.284(-1)	0.450	0.103
3	0.319(-1)	0.321(-1)	0.311(2)	0.117(1)	0.340(1)	0.170	0.459(1)	0.191(1)	0.282(1)
4	0.679(-1)	0.506	0.903(-1)	0.157(1)	0.104	0.151	0.213	0.169	0.796(-1)
5	0.508(-1)	0.201	0.113(1)	0.450	0.415(1)	0.103(1)	0.169(1)	0.113(1)	0.871(-1)
6	0.219(-1)	0.448	0.131(-1)	0.150	0.235	0.164(1)	0.647(-1)	0.399(-1)	0.183(-2)
7	0.412(-1)	0.415(-1)	0.153(1)	0.928	0.169(1)	0.282	0.335(1)	0.105	0.233
8	0.296(-1)	0.391	0.383	0.440	0.679	0.105	0.620(-1)	0.800(1)	0.283
9	0.807(-2)	0.890(-1)	0.562	0.208	0.523(-1)	0.468(-2)	0.139	0.283	0.116(2)
$E_1 = 0.93\text{Ry}, {}^3S^e, p = -1$									
1	0.178(1)	0.484(-1)	0.853(-2)	0.158(-1)	0.603(-2)	0.167(-1)	0.457(-2)	0.191(-2)	0.625(-3)
2	0.247	0.235(2)	0.390	0.109(1)	0.435	0.294(1)	0.163(1)	0.171(1)	0.182(1)
3	0.193	0.170(1)	0.514(2)	0.892(1)	0.208(1)	0.105(2)	0.167(2)	0.596	0.381(1)
4	0.277(-1)	0.362	0.683	0.846	0.576	0.801	0.344(-1)	0.924(-2)	0.920(-1)
5	0.453(-1)	0.633	0.695	0.251(1)	0.373(2)	0.525	0.348(1)	0.295(1)	0.367(1)
6	0.291(-1)	0.981	0.810	0.804	0.121	0.416(1)	0.887(-1)	0.121	0.803(-1)
7	0.333(-1)	0.236(1)	0.556(1)	0.151	0.348(1)	0.388	0.276(2)	0.290(1)	0.186(1)
8	0.831(-2)	0.149(1)	0.119	0.240(-1)	0.177(1)	0.315	0.174(1)	0.448(1)	0.280(1)
9	0.259(-2)	0.158(1)	0.760	0.241	0.220(1)	0.208	0.111(1)	0.280(1)	0.935(1)

TABLE VII: The same as in Table VI at channel energy $E_1 = 0.91\text{Ry}$.

Ch.#	1	2	3	4	5	6	7	8	9
$E_1 = 0.91\text{Ry}, {}^1S^e, p = +1$									
1	0.365(-2)	0.102(-1)	0.102(-2)	0.437(-1)	0.474(-2)	0.137(-1)	0.397(-2)	0.521(-2)	0.154(-2)
2	0.576(-1)	0.218(1)	0.648(-2)	0.185(1)	0.395	0.122(1)	0.694(-1)	0.109	0.276(-1)
3	0.428(-1)	0.485(-1)	0.963(2)	0.213(1)	0.380(1)	0.262	0.107(1)	0.683(1)	0.517(1)
4	0.829(-1)	0.617	0.954(-1)	0.193(1)	0.155	0.245	0.206	0.989(-1)	0.279(-1)
5	0.666(-1)	0.981	0.127(1)	0.115(1)	0.509(1)	0.605	0.326(1)	0.168(1)	0.944
6	0.261(-1)	0.408	0.118(-1)	0.246	0.818(-1)	0.188(1)	0.367(-1)	0.139	0.520(-1)
7	0.563(-1)	0.174	0.356	0.153(1)	0.326(1)	0.271	0.570(1)	0.157(1)	0.262(1)
8	0.444(-1)	0.163	0.137(1)	0.443	0.101(1)	0.616	0.940	0.160(2)	0.438
9	0.133(-1)	0.411(-1)	0.103(1)	0.125	0.567	0.232	0.157(1)	0.438	0.187(2)
$E_1 = 0.91\text{Ry}, {}^3S^e, p = -1$									
1	0.182(1)	0.438(-1)	0.788(-2)	0.1567(-1)	0.605(-2)	0.159(-1)	0.450(-2)	0.209(-2)	0.633(-3)
2	0.243	0.241(2)	0.209(1)	0.170(1)	0.126(1)	0.479(1)	0.106(1)	0.632	0.652
3	0.329	0.156(2)	0.166(3)	0.888(1)	0.146(1)	0.851(1)	0.334(1)	0.471(1)	0.797(1)
4	0.296(-1)	0.567	0.397	0.139(1)	0.464	0.102(1)	0.119	0.123	0.107
5	0.846(-1)	0.311(1)	0.486	0.345(1)	0.814(2)	0.524	0.604(1)	0.480	0.144(1)
6	0.296(-1)	0.160(1)	0.382	0.102(1)	0.706(-1)	0.445(1)	0.192	0.177	0.140
7	0.632(-1)	0.263(1)	0.111(1)	0.885	0.604(1)	0.143(1)	0.540(2)	0.255	0.113(1)
8	0.179(-1)	0.943	0.942	0.550	0.2895	0.793	0.153	0.633(1)	0.231(1)
9	0.551(-2)	0.971	0.159(1)	0.480	0.8620	0.627	0.676	0.231(1)	0.218(2)

TABLE VIII: The same as in Table VI at channel energy $E_1 = 0.89\text{Ry}$.

Ch.#	1	2	3	4	5	6	7	8	9
$E_1 = 0.89\text{Ry}, {}^1S^e, p = +1$									
1	0.342(-2)	0.940(-2)	0.819(-3)	0.474(-1)	0.262(-2)	0.154(-1)	0.264(-2)	0.292(-2)	0.849(-3)
2	0.609(-1)	0.252(1)	0.412(-1)	0.212(1)	0.693(-1)	0.108(1)	0.976(-1)	0.777(-1)	0.306(-1)
3	0.466	0.361(1)	0.550(3)	0.862(1)	0.384(2)	0.567(1)	0.177(3)	0.672(2)	0.232(2)
4	0.102	0.708	0.326(-1)	0.233(1)	0.126	0.422	0.109	0.136	0.363(-1)
5	0.495	0.205(1)	0.128(2)	0.111(2)	0.400(3)	0.264(1)	0.166(1)	0.123(2)	0.510(2)
6	0.327(-1)	0.361	0.213(-1)	0.422	0.302(-1)	0.223(1)	0.468(-1)	0.366(-1)	0.133(-1)
7	0.500	0.286(1)	0.591(2)	0.965(1)	0.166(1)	0.415(1)	0.106(3)	0.146(1)	0.291(2)
8	0.331	0.138(1)	0.135(2)	0.719(1)	0.735(1)	0.193(1)	0.879	0.695(2)	0.302(2)
9	0.965(-1)	0.538	0.464(1)	0.192(1)	0.306(2)	0.706	0.175(2)	0.302(2)	0.140(3)
$E_1 = 0.91\text{Ry}, {}^3S^e, p = -1$									
1	0.186(1)	0.408(-1)	0.669(-2)	0.170(-1)	0.571(-2)	0.158(-1)	0.287(-2)	0.160(-2)	0.258(-3)
2	0.267	0.277(2)	0.983(-1)	0.972	0.415	0.398(1)	0.188(1)	0.309(1)	0.174(1)
3	0.376(1)	0.862(1)	0.175(4)	0.264(3)	0.235(3)	0.266(3)	0.115(3)	0.886(2)	0.392(3)
4	0.360(-1)	0.324	0.996	0.345(1)	0.563	0.698	0.542(-1)	0.574(-1)	0.483(-1)
5	0.108(1)	0.122(2)	0.785(2)	0.498(2)	0.796(3)	0.440(2)	0.186(3)	0.273(2)	0.202(2)
6	0.337(-1)	0.133(1)	0.101(1)	0.698	0.500	0.707(1)	0.227(-2)	0.105	0.151
7	0.554	0.553(2)	0.382(2)	0.482(1)	0.185(3)	0.193	0.233(3)	0.694(2)	0.754(2)
8	0.189	0.544(2)	0.177(2)	0.303(1)	0.164(2)	0.557(1)	0.416(2)	0.106(3)	0.980(2)
9	0.314(-1)	0.307(2)	0.784(2)	0.253(1)	0.121(2)	0.799(1)	0.453(2)	0.981(2)	0.26(3)